Long title: Genetic isolation by distance underlies color pattern divergence in red-eyed treefrogs (*Agalychnis callidryas*)

Short title: IBD and color pattern in red-eyed treefrogs

Authors: Meaghan I. Clark[1,2,3*], Gideon S. Bradburd[2], Maria Akopyan[1,4], Andres Vega[5], Erica Bree Rosenblum[6,7] & Jeanne M. Robertson[1,8]

[1] Department of Biology, California State University Northridge, Northridge, CA, USA
[2] Department of Integrative Biology, Ecology, Evolution and Behavior Group, Michigan State University, East Lansing, Michigan
[3] W.K. Kellogg Biological Station, Michigan State University, Hickory Corners, MI, USA
[4] Department of Ecology and Evolutionary Biology, Cornell University, Ithaca, NY, USA
[5] AMBICOR, Tibas, Costa Rica
[6] Department of Environmental Science, Policy, and Management, University of California Berkeley, Berkeley, CA, USA
[7] Museum of Vertebrate Zoology, University of California Berkeley, Berkeley, CA, USA
[8] Department of Herpetology, Natural History Museum of Los Angeles County, Los Angeles, CA, USA

[*] corresponding author; clarkm89@msu.edu

Abstract

Investigating the spatial distribution of genetic and phenotypic variation can provide insights into the evolutionary processes that shape diversity in natural systems. We characterized patterns of genetic and phenotypic diversity to learn about drivers of color-pattern diversification in red-eyed treefrogs (*Agalychnis callidryas*) in Costa Rica. Along the Pacific coast, red-eyed treefrogs have conspicuous leg color patterning that transitions from orange in the north to purple in the south. We measured phenotypic variation of frogs across Pacific sites, with increased sampling at sites where the orange-to-purple transition occurs. At the transition zone, we discovered the co-occurrence of multiple color-pattern morphs. To explore possible causes of this variation, we generated a SNP dataset with RAD sequencing to analyze population genetic structure, measure genetic diversity, and infer the processes that mediate genotype-phenotype dynamics. We investigated how patterns of genetic relatedness correspond with individual measures of color pattern along the coast, including testing for the role of hybridization in geographic regions where orange and purple phenotypic groups co-occur. We found no evidence that color-pattern polymorphism in the transition zone arose through recent hybridization or introgression. Instead, a strong pattern of genetic isolation by distance (IBD) indicates that color-pattern variation was retained through other processes such as ancestral color polymorphisms, ancient secondary contact or generated by novel mutations. We found that color phenotype changes along the Pacific coast more than would be expected from geographic distance alone. Combined, our results suggest the possibility of selective pressures acting on color pattern at a small geographic scale.

Keywords

Population genetics, color-pattern polymorphism, introgression, Costa Rica

Introduction

A central goal of evolutionary biology is to understand how phenotypic variation is generated, distributed, and maintained in natural systems (Mayr, 1963; Mitchell-Olds et al., 2007). Color pattern is a phenotype well-suited for evolutionary study because it is easily quantifiable and often has adaptive value (Cott, 1940; Orteu & Jiggins, 2020). Many compelling examples of natural selection in the wild have come from studying color-pattern variation across diverse empirical systems (e.g. Corl et al., 2010; Hoekstra et al., 2004; Lowry et al., 2012; Maan et al., 2008; Pfeifer et al., 2018; Rosenblum et al., 2006; Streisfeld & Kohn, 2005; Supple et al., 2015; Twomey et al., 2015). In animals, color and color pattern play important ecological roles, for example as a deterrent to predation (crypsis, aposematism), as a signal to conspecifics (mate choice, territoriality), or both (Cummings & Crothers, 2013; Rojas, 2016; Selz et al., 2016; Stevens & Merilaita, 2009). Accordingly, color and color pattern are often shaped by selection, and variation in color traits can provide insight into the evolutionary dynamics that shape diversity. Color variation within a species can be distributed at a regional level with little variation within sites (polytypic), found at a single locality (polymorphic), or both (e.g., Wang & Summers, 2010). The distribution of color variation within species can provide particular insight on the spatial scale over which evolutionary dynamics act (Svensson, 2017).

Quantifying the distribution of phenotypic and genetic variation in color polytypic and/or polymorphic species can provide insights into the processes maintaining phenotypic variation on a microevolutionary scale. A variety of evolutionary scenarios could explain polytypic and polymorphic patterns of variation. For example, polytypic variation can persist when there is limited gene flow among populations due to environmental, geographic, or reproductive barriers or selection against maladapted migrants (Endler, 1973; Lehtonen et al., 2009; Rosenblum et al., 2006, 2010). Conversely, little variation across populations is expected when there is substantial gene flow among morphs or if color is under stabilizing selection (Duftner et al., 2006; Slatkin, 1985). Polymorphic variation within populations can arise through novel mutations, contemporary gene flow, the retention of ancestral polymorphism, and/or ancient secondary contact (Lim et al., 2010; Roland et al., 2017). Polymorphism often occurs at transition zones between distinct morphs (Planes & Doherty, 1997). In such contact zones, hybridization could increase phenotypic variation if hybrids have novel color phenotypes (Akopyan et al., 2020b; Anderson & Stebbins, 1954). While quantifying color-pattern variation can be straight-forward, determining the underlying evolutionary processes that generate and/or maintain variation presents a challenge and an opportunity to understand phenotypic evolution in natural systems.

The striking color-pattern variation of red-eyed treefrogs, *Agalychnis callidryas* Cope 1862, provides an excellent system in which to study the mechanisms of extreme phenotypic variability. Red-eyed treefrogs are distributed from central Mexico to northern Colombia (Campbell, 1999; Savage & Heyer, 1967) and are variable in flank and leg color-pattern across their range (Robertson & Robertson, 2008; Robertson & Zamudio, 2009). Flank and leg color are not sexually dimorphic, do not change within individuals as a response to light intensity (Schliwa & Euteneuer, 1983) and are known to be heritable based on breeding studies (J.M. Robertson,

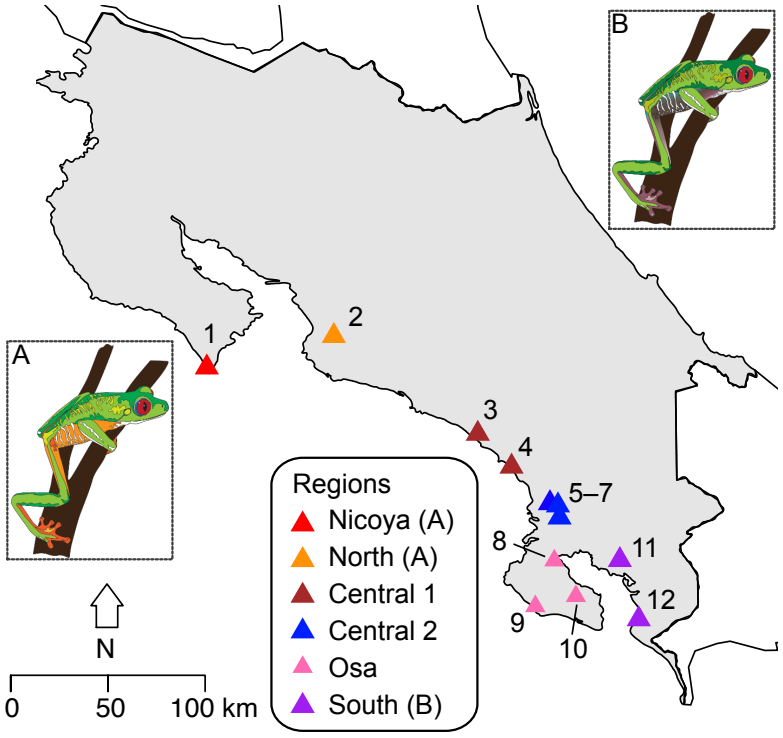

Figure 1. Map indicating the 12 sampling sites for red-eyed treefrogs (*Agalychnis callidryas*) along the Pacific coast of Costa Rica. Each site is assigned to one of six biogeographic regions: Nicoya, north, central 1, central 2, Osa, and south. Insets A and B: red-eyed treefrog (*Agalychnis callidryas*) color morphs, drawn from photographs, illustrate color patterns typical of northern orange (A) and southern purple (B) regions (illustrations: Cynthia J. Hitchcock).

unpublished data). Four distinct flank and leg color morphs exist in Costa Rica and Panama: blue, red/blue, orange, or purple (Robertson & Robertson, 2008). Across their range, red-eyed treefrogs are polytypic, but generally not polymorphic (Robertson & Robertson, 2008; Robertson & Vega, 2011), except in a narrow contact zone on the Caribbean slope of Costa Rica (Akopyan et al., 2020b). Flank and leg color-pattern likely evolve through both sexual selection due to preference for local morphs during mate choice (Akopyan et al., 2018; Jacobs et al., 2016; Kaiser et al., 2018) and natural selection for color pattern to potentially act as a warning signal to predators (Davis et al., 2016; Robertson & Greene, 2017, Clark unpublished). Thus, the evolutionary dynamics and impacts of selection have likely shaped the polytypic and polymorphic distributions of color pattern in red-eyed treefrogs.

We focused on populations of red-eyed treefrogs from mainland and peninsular populations of the Pacific slope of Costa Rica. Red-eyed treefrogs on the Pacific and Caribbean slopes are isolated from one another by the Cordillera de Talamanca (Robertson & Zamudio, 2009). On the Pacific slope, color variation is characterized by a north-south gradient: in the north, frogs generally have orange flanks and legs (orange morph), while in the south, they display purple flanks and legs (purple morph, Fig. 1). Previous work on Pacific populations revealed a complex relationship between geography, color pattern, mitochondrial and nuclear markers (Robertson et al., 2009). Within the Pacific slope, northern and southern sites do not share mitochondrial haplotypes, except at a single centrally located site (Robertson and Zamudio 2009; Fig. 1, Site 4; Table 1). The Pacific slope is geographically and environmentally complex:

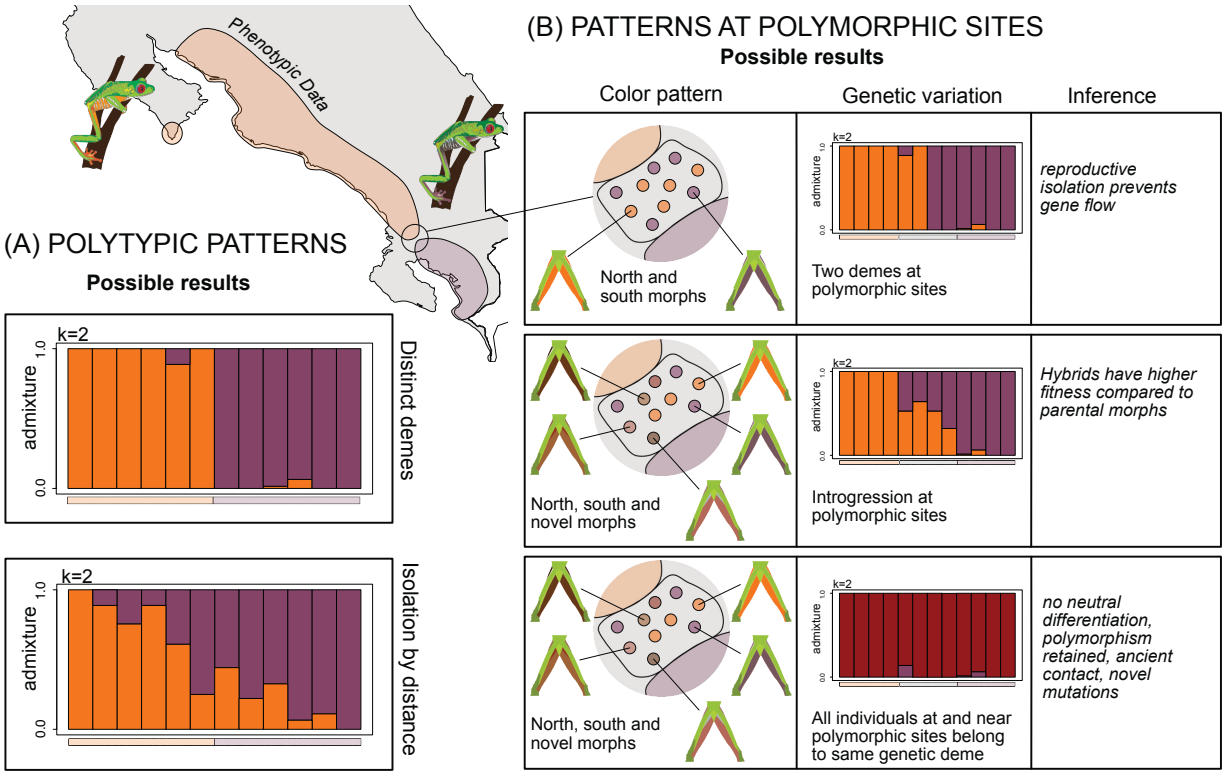

Figure 2. Hypotheses and predictions tested by this study. (A) Genetic predictions based on the polytypic color-pattern distribution of two color morphs on the Pacific slope of Costa Rica. (B) Possible genetic and phenotypic outcomes and inferences when considering the transition zone where polymorphism is observed.

two peninsulas, the Nicoya and Osa, are potentially isolated from mainland sites through geographic barriers and inhospitable habitat (Robertson et al., 2009). Recent field sampling efforts identified polymorphic sites where color pattern transitions from the orange to the purple morph (Central 2, Fig. 1). We aim to understand the evolutionary processes underlying both polytypic and polymorphic color-pattern distributions on the Pacific coast.

In this study, we document the distribution of polytypic and polymorphic color patterns across the orange-purple color-pattern gradient and combine those data with a genomic dataset generated using RAD-seq to understand the evolutionary mechanisms that generate and maintain patterns of diversity. We expanded sampling from previous studies to examine genomic ancestry across and within orange, purple, and polymorphic sites to determine whether recent hybridization explains polymorphism in the transition zone. We expected our data to support one of two hypotheses regarding polytypic patterns: (1) purple and orange morphs represent distinct genetic demes, consistent with selection for premating reproductive isolation among these morphs (Akopyan et al., 2018), or alternatively, (2) samples along the coast are characterized by a pattern of genetic isolation by distance (IBD) that is not correlated with phenotypic variation, which could indicate local selection acting to maintain color morphs (Fig. 2A). At polymorphic sites in the transition zone, we combine analyses of color pattern, genetic variation, and relatedness to infer if either (1) reproductive isolation prevents gene flow between orange and purple morphs, as evidenced by distinct parental groups and a lack of hybrid individuals, (2) polymorphic sites represent a contact zone between orange and purple morphs, with genetic

hybrids and novel color patterns present, or (3) orange, purple, and novel morphs are present at polymorphic sites, but with no genetic differentiation between morphs at neutral markers. This third scenario would suggest that either color-pattern polymorphism was retained from an ancestral population, there has been ancient secondary contact, or that novel morphs have been generated by new mutations (Fig. 2B). Integrating analyses of variation at both large (polytypic) and small (polymorphic) scales, we are able to illuminate how color pattern evolves at microgeographic scales.

Methods

Field sampling and study sites

Our study focused on 12 sites along the Pacific coast of Costa Rica, west of the continental divide (Fig 1). Previous studies characterized red-eyed treefrogs at northern sites (Sites 1–8) as orange and at a southern site as purple (Site 12) (Robertson & Vega, 2011). Here, we expanded previous geographic sampling (Robertson et al., 2009) by adding six sites to assess fine-scale variation in phenotype and genotype, including: the central coast (Site 3), the Osa Peninsula (Sites 9 and 10), mainland adjacent to Osa Peninsula (Sites 5 and 6), and Gulfo Dulce (Site 11). We included 9–25 individuals from previously sampled sites, and 3–20 individuals from new sites (Table 1). We bred frogs from Site 2 with frogs from Site 12 in captivity at California State University, Northridge (IACUC 1819-005) to produce F1 hybrids to serve as controls in ancestry analyses (see genomic analyses below).

We grouped sites together into six regions based on potential geographic barriers, and divisions between phenotypic and known genetic groups (Fig. 1). The Nicoya Peninsula (Site 1) is geographically isolated from all mainland populations by dry forest, which is an unsuitable habitat for red-eyed treefrogs. The Central 1 (Sites 3-4) region is separated from the North (Site 2) based on distinct mtDNA haplotypes (Robertson & Zamudio, 2009). The Central 2 region (Sites 5-7) contains both orange and purple frogs whereas frogs in the South (Sites 11-12) only have purple legs. The Terraba and Sierpe Rivers separate the Osa Peninsula (Sites 8–10) from the mainland (Kohlmann et al., 2002; Robertson & Vega, 2011).

Table 1. Location, geographic coordinates, sample size, mtDNA clade (Robertson & Zamudio, 2009) and genetic diversity for 12 sampling sites of red-eyed treefrogs (*Agalychnis callidryas*) along the Pacific coast of Costa Rica. MtDNA haplotype not identified (—) for some sites. Estimates of nucleotide diversity (π) and Wu and Watterson's theta (θ_w) based on RADseq dataset. See Fig. 1 for region designations.

#	Site	Province	Region	Latitude (N)	Longitude (W)	*n*	mtDNA clade	π	θ_w
1	Cabo Blanco	Guanacaste	Nicoya	9.5805	-85.1246	9	B	0.088	0.071
2	Bijagual	San Jose	North	9.7256	-84.5313	9	B	0.154	0.131
3	Firestone	Puntarenas	Central 1	9.274927	-83.8589	3	—	0.167	0.126
4	Uvita	Puntarenas	Central 1	9.1235	-83.7011	5	A, B	0.165	0.149
5	Cortes	Puntarenas	Central 2	8.95517	-83.52177	12	—	0.169	0.152
6	Palmar Sur	Puntarenas	Central 2	8.94488	-83.48444	20	—	0.168	0.144
7	Sierpe	Puntarenas	Central 2	8.8892	-83.477	17	A	0.174	0.163
8	El Campo	Puntarenas	Osa	8.6909	-83.5013	17	A	0.163	0.144
9	Sirena	Puntarenas	Osa	8.480261	-83.59012	19	—	0.165	0.145
10	El Tigre	Puntarenas	Osa	8.52678	-83.40053	19	—	0.165	0.143
11	Gamba	Puntarenas	South	8.69333	-83.19522	19	—	0.164	0.143
12	Pavones	Puntarenas	South	8.4204	-83.1069	25	A	0.161	0.138

At each site, we captured frogs by hand and took digital photographs with a black-white-gray standard (QPcard 101, Adorama Camera Inc., New York, New York) of the posterior aspect of their legs (for samples collected before 2015, see Robertson & Robertson 2008, Robertson & Vega 2011; for samples collected in 2015 see Akopyan et al. 2020b) We obtained a toe clip for genomic analyses, which was stored in 100% ethanol. Frogs were released within one day at the site of capture. We also took a toe clips from eight lab-bred F1 hybrids.

Quantifying color pattern

Photos were color corrected in Photoshop CC v. 18.0.0 (Adobe, San Jose, CA) using the black-white-gray standard. To quantify color pattern, we focused on the posterior leg because leg and flank color-pattern were found to be strongly correlated in previous work (Robertson & Robertson, 2008). The colored region of the frogs' legs can be either uniform in color or contain a gray/blue patch on the inner leg (Suppl. Fig. 1). In all cases, we excluded the patch and selected the colored region of one leg and used the average function in Photoshop to measure hue, saturation, and brightness (Adobe, San Jose, CA). Because orange and purple have similar hue values, the saturation and brightness values were useful to distinguish color pattern within and among populations (Robertson & Robertson, 2008). We used ImageJ (Abràmoff et al., 2005) to quantify the percent of pixels on the leg that were covered by the gray patch, which was easily distinguished from the dominant portion of the leg using saturation values.

We used principal component analysis (PCA) in R v. 3.5.3 (R Core Team 2016) based on hue, saturation, brightness, and percent gray of the hind legs to visualize the distribution of color variation among red-eyed treefrog populations within and among regions. We conducted a discriminant function analysis (DFA) using the MASS package in R v. 3.5.3. to test whether individuals were correctly assigned to their site of origin based on hue, saturation, brightness, and percent gray.

Table 2. Discriminant function analysis of leg color pattern for 12 sampling sites of red-eyed treefrogs (*Agalychnis callidryas*) along the Pacific coast of Costa Rica. Each individual was classified based on its leg color pattern and assigned to a sampling site.

		Region of Origin											
		Nicoya	North	Central 1		Central 2			Osa			South	
		1	2	3	4	5	6	7	8	9	10	11	12
Classification	1	100%	0	0	0	0	0	24%	6%	0	0	0	0
	2	0	22%	67%	0	8%	0	6%	6	0	0	0	0
	3	0	0	0	0	0	0	0	0	0	0	0	0
	4	0	0	0	100%	0	0	6%	0	0	0	0	0
	5	0	22%	33%	0	69%	15%	0	0	0	0	0	0
	6	0	0	0	0	15%	65%	6%	12%	0	0	0	0
	7	0	11%	0	0	8%	15%	41%	18%	0	0	0	0
	8	0	33%	0	0	0	0	12%	59%	0	0	0	0
	9	0	11%	0	0	0	0	6%	0	95%	0	0	20%
	10	0	0	0	0	0	5%	0	0	0	74%	25%	0
	11	0	0	0	0	0	0	0	0	0	26%	75%	4%
	12	0	0	0	0	0	0	0	0	5%	0	0	76%

Molecular methods

DNA was extracted from frog toe clips using a DNeasy Blood and Tissue kit (Qiagen, Valencia, CA) per the manufacturer's protocol, except as described below. We eluted DNA in 50 uL AE to increase concentration. After extraction, 4 uL of 1 mg/mL RNAse A was added to each sample to remove RNA contamination. DNA concentration was measured using a Qubit 2.0 Fluorometer (ThermoFisher, Waltham, MA). Restriction site associated DNA sequencing (RAD-seq) libraries (Ali et al., 2016; Etter et al., 2011) containing samples from 12 sites and eight lab-bred F1 hybrids were prepared with restriction enzyme sbf1. We included 4 to 20 individuals per site (Table 1). Libraries were sequenced on one lane of a HiSeq4000 (PE 150; Illumina San Diego, California).

Quality filtering and SNP calling

We processed RAD-seq data as in Akopyan et al. (2020). Briefly, raw reads with the cut site on the reverse read were rescued using a custom Perl script. The *clone_filer* program in STACKS (Catchen et al., 2013) was used to remove PCR clones. Sequence data were demultiplexed using the *process_radtags* function in STACKS. Reads containing base pairs with a phred score less than 10 were removed. We used *ustacks* in STACKS for *de novo* assembly, requiring a minimum of three reads to create a stack, and a maximum of four base-pair differences between stacks. A pseudo-reference genome was created using a custom Perl script. Over half of the individuals had to have a stack for it to be used in the pseudo-reference genome. Reads were aligned to the pseudo-reference genome using the program BWA v. 0.7.15-r1142 (Li & Durbin, 2009). Samtools v. 1.9 (Li et al., 2009) was used to index, sort, and merge alignments. We used Bcftools v. 1.3.1 (Li, 2011) to call variants and create a VCF file. The data were filtered using a custom Perl script to retain a single SNP per contig. Loci with mean allele frequencies <0.5% and individuals with >70% missing data were not included in subsequent analyses. Pipeline and scripts are available online (Akopyan et al., 2020a).

Population genomic analyses

We calculated measures of genetic variability, population pi (π) at polymorphic sites, and Wu and Watterson's theta (θ_w, Watterson 1975), in R using custom scripts. Bayesian clustering methods in the program entropy (Gompert et al., 2014) were used to estimate admixture proportions and interpopulation ancestry. We excluded sites 1 and 8–10 from the entropy analysis to limit the dataset to putative parental and hybrid groups based on admixture proportions. To assess the possibility of hybridization across sites, we plotted interpopulation ancestry (Q_{12}) against admixture proportion (q) (Gompert & Buerkle, 2016). Interpopulation ancestry, the proportion of an individual's genome where each allele at a locus is from a different putative parental group, separates out F1 hybrids (Q_{12} near 1), multigenerational hybrids (intermediate Q_{12}) and individuals with late-stage hybrid genomes (Q_{12} near 0). The lab-reared F1 hybrids served as a useful control for what we expect for F1 hybrids. Multigenerational hybrids were expected to show elevated interpopulation ancestry, but below that of F1 hybrids.

We ran Mantel tests in R package ade4 (10,000 replicates) to test for patterns of genetic and phenotypic IBD and for a relationship between genetic and phenotypic distance (Chessel et al., 2004). We assumed frogs would avoid crossing bodies of saltwater, so we calculated distances among populations as over-land geographic distances. We calculated pairwise F_{ST} between sites in the R package BEDASSLE (Bradburd et al., 2013; Weir & Hill, 2002). To calculate the genetic distance among individuals, we conducted a PCA in R using our genomic

SNP data, and calculated the Euclidean distance among the first four axes of the principal components (Shirk et al., 2017). Increasing the number of principal components used did not change test results. We estimated phenotypic distance by calculating the pairwise Euclidean distance of hue, saturation, brightness, and percent gray. A Q_{ST}–F_{ST} or P_{ST}–F_{ST} approach is not justified for this study because we did not measure phenotype in a common garden, and the genetic basis of color pattern in red-eyed treefrogs is unknown (Pujol et al., 2008).

Because we observed a strong pattern of genetic IBD (see Results), we used the R package conStruct to assess genetic clustering while accounting for divergence resulting from geographic distance (Bradburd et al., 2018). The spatial model in conStruct estimates admixture proportions for each sample while simultaneously accounting for decay in genetic relatedness with distance within each genetic grouping. We ran spatial and non-spatial models using K-values one through seven. We assessed the biological importance of each added K-value by (1) comparing the contribution of each layer to overall covariance, (2) cross validation analysis that compares the predictive accuracy of models using eight replicates and 1000 iterations, and (3) assessing the biological realism of the model given previous knowledge of the system.

To evaluate phenotypic patterns while accounting for genetic relatedness, we fit three sets of Bayesian models implemented in rstan (Stan Development Team, 2018): (1) we modeled individual phenotype measurements (hue, saturation, brightness, and PC1) each as a function of latitude, (2) we modeled the average phenotype for each site as a function of latitude, and (3) we modeled phenotypic variation at a site as a function of latitude or θ_w. All models included a covariance structure that was a function of the genetic relatedness between individuals. We used

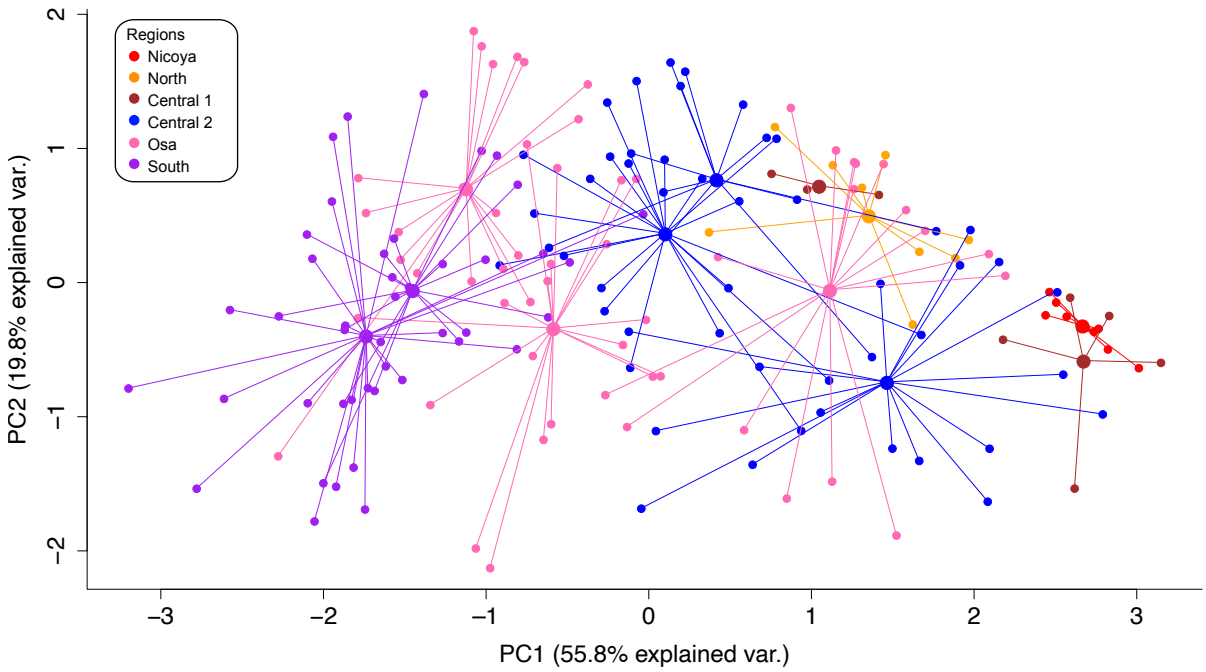

Figure 3. Principle component analysis of leg phenotype for red-eyed treefrogs (*Agalychnis callidryas*) sampled from 12 sites along the Pacific coast of Costa Rica. Lines connect individuals (small dots) with the mean phenotype of each sampling site (large dots). Individuals and means are color coded by region.

latitude as a proxy for a site's location along the Pacific coast. These models allowed us to detect variation in phenotype above and beyond that explained by covariance at putatively neutral genetic markers.

Results

Phenotypic variation

Phenotypic patterns along the Pacific coast matched previous studies: frogs had orange legs and flanks in the northern regions and purple flanks and legs in the south. We confirmed that the three sites in the Central 2 region were polymorphic. The first two principal components in our PCA explained 75.6% of the total variance in measured leg color metrics (Fig. 3). Sites in the Nicoya, North and Central 1 regions (orange legs) formed one cluster in phenotypic space, and sites in the South (purple legs) formed another. Sites in the Central 2 region were generally intermediate, but closer to the orange cluster. Osa sites were variable: Site 10 clustered with the purple/south sites, Site 8 clustered with the orange/northern sites, and Site 9 was intermediate. The DFA revealed three phenotypic groups (Table 2). Individuals from the Nicoya had 100% correct assignment. The majority of frogs were correctly assigned to their region of origin, with the exception of orange frogs, which were frequently assigned to phenotypically similar sites (Table 2). Frogs from polymorphic sites in the Central 2 region also had high misclassification probabilities (Table 2). Most (72.7%) purple individuals from the South were assigned to the correct region. Over half of the individuals from the Osa were assigned to the correct site;

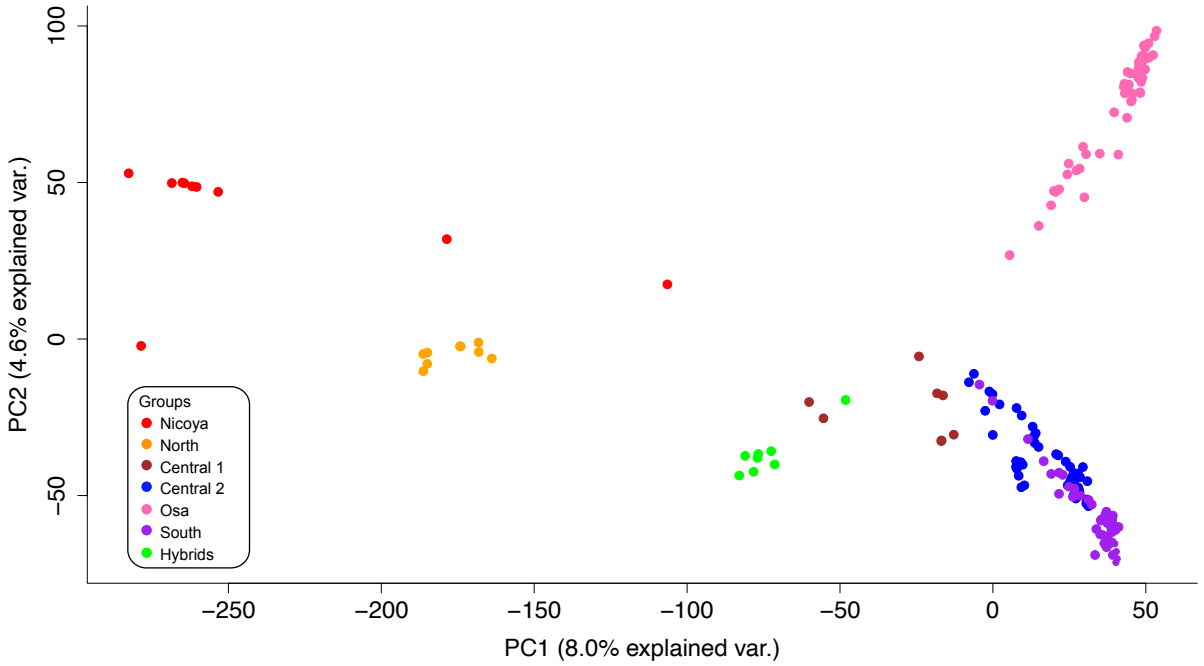

Figure 4. Principle component analysis of genomic SNPs for red-eyed treefrogs (*Agalychnis callidryas*) sampled from 12 sites along the Pacific coast of Costa Rica. Dots represent individuals and are color coded by region. Green dots are lab generated hybrids between Site 2 and Site 12.

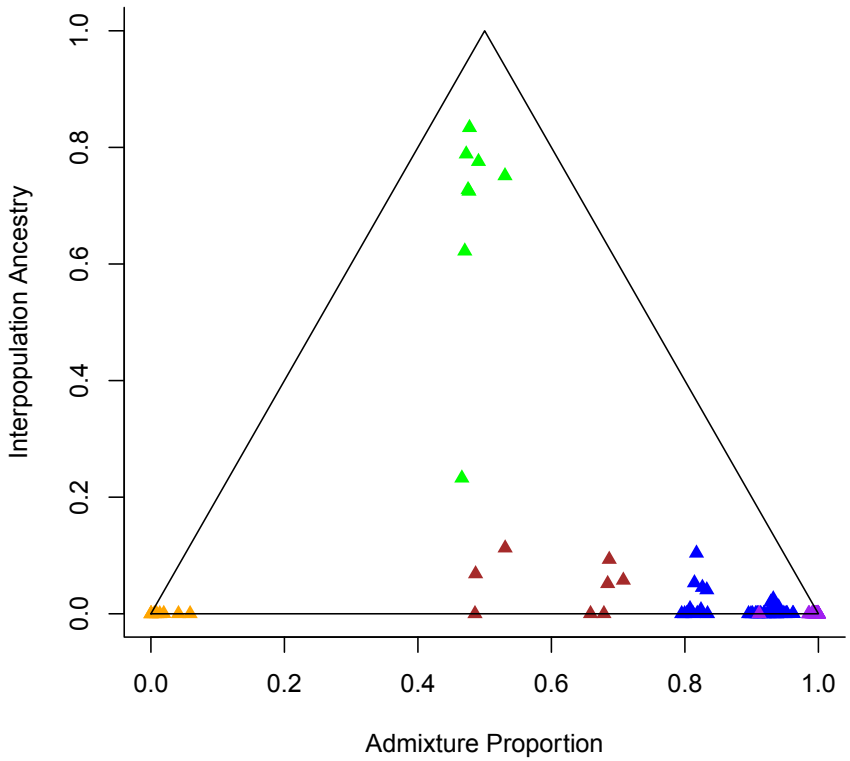

Figure 5. Scatterplot of admixture proportion (q) and interpopulation ancestry (Q_{12}), the proportion of an individual's genome where one allele is assigned to each parental group, for red-eyed treefrogs (*Agalychnis callidryas*) sampled from 5 sites along the Pacific coast of Costa Rica. Dots represent individuals and are color coded by region (see Fig. 1 legend). Only lab generated hybrids (green) show high interpopulation ancestry indicative of hybrid origin.

misclassified individuals were most often assigned to sites with color patterns similar to their respective Osa site (e.g., 26% of purple morph frogs from Site 10 were misassigned to Site 11, another purple morph site).

Genetic variation

After filtering, we retained 71,746 SNPs in 174 individuals. The mean coverage per SNP was 9.3X. Descriptive statistics indicated similarity in genetic diversity among sites, with the exception of Site 1, which had lower genetic diversity (Table 1). Pairwise F_{ST} values ranged from 0.025 to 0.412 (Table 3). The PCA revealed genetic clustering corresponding to geographic regions (Fig. 4). Combined, the first two principal components explained 12.6% of variation. The Nicoya, North, Central 1, the Osa, and the lab-generated hybrids were genetically distinct, while South and Central 2 regions clustered together.

The comparison of admixture proportion (q) and interpopulation ancestry (Q_{12}) from entropy showed no evidence of hybridization when parental populations were assigned as North and South. Lab-generated hybrids had intermediate admixture proportions and high interpopulation ancestry scores, as expected. No wild frogs had elevated interpopulation ancestry scores (Fig. 5).

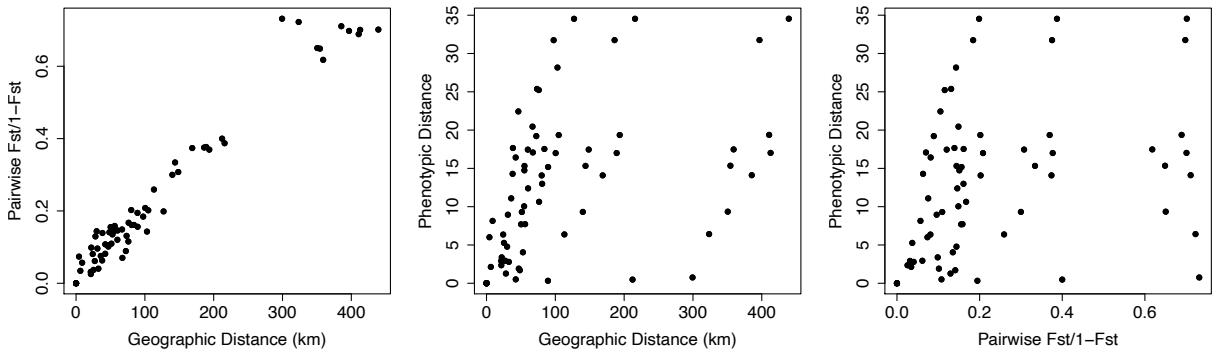

Figure 6. Relationship between over-land geographic distance and genetic distance for 12 sites of red-eyed treefrogs (*Agalychnis callidryas*) along the Pacific coast of Costa Rica. There is a strong positive relationship between geographic and genetic distance, suggesting a pattern of isolation by distance (r = 0.965, $p < 0.001$); however, the relationships between phenotypic and geographic distance ($r = 0.368$, $p < 0.062$) and genetic and phenotypic distance ($r = 0.310$, $p = 0.088$) were considerably weaker.

Genotypic and phenotypic patterns

Mantel tests revealed a strong positive relationship between geographic and genetic distance (r = 0.965, p <0.001) and weak positive relationships between geographic and phenotypic distance (mantel test, $r = 0.368$, $p = 0.062$) and genetic and phenotypic distance (mantel test, $r = 0.310$, $p = 0.088$).

The R package conStruct quantified genetic clustering while accounting for geographic distance. Compared to both conStruct's non-spatial model and entropy, conStruct's spatial model inferred fewer discrete genetic clusters (Fig. 7). Cross-validation analysis showed that spatial models have better predictive accuracy than non-spatial models (Suppl. Fig. 5). Although each additional layer from K=1 to 7 increased the predictive accuracy of the model (Suppl. Fig 6.), layer contributions decreased dramatically after K = 2 (Suppl. Fig. 6). All spatial models with K ≥ 2 assigned groups on the Nicoya and Osa peninsulas to the same cluster. There is no obvious biological explanation for why the populations at these sites would be assigned to the same discrete cluster. It is likely that runs at K ≥ 2 are describing the genetic dissimilarity between frogs on the Nicoya and Osa peninsulas with the IBD component of the model within a single layer. This may not reflect recent shared ancestry, and instead may be an artifact of the large geographic distance between these locations combined with gaps in our sampling. Therefore, we interpret K = 1 as the model with the most biological significance.

We used Bayesian models to evaluate relationships between phenotypic measurements (PC1, hue, saturation and brightness) and latitude while accounting for genetic covariance. Using 95% credible intervals, with a Dunn-Bonferroni correction for multiple tests, we found that individual leg saturation, hue, and PC1, but not brightness, vary significantly with latitude while accounting for genetic covariance among sampled individuals (Fig. 8). These correlations are not significant when using phenotypic averages for each site. We did not find significant relationships between variation in phenotypic measures and θ_w, or latitude.

Polytypic patterns: Pattern of isolation by distance found across polytypic regions

Most of the genetic variation among red-eyed treefrogs populations is explained by over-land distance among sites; orange and purple morphs do not represent separate genetic demes (Fig.

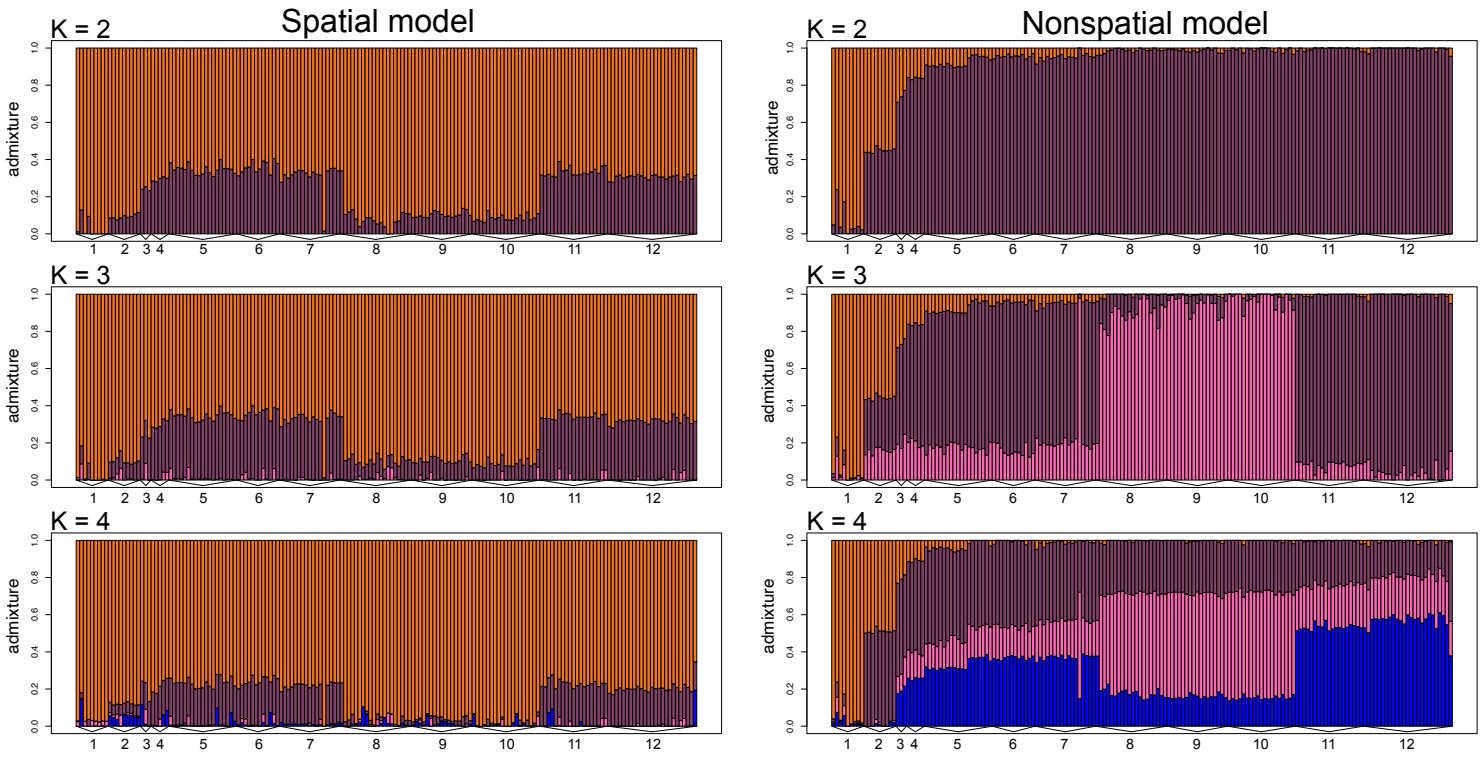

Figure 7. Barplots of admixture proportions for red-eyed treefrogs (*Agalychnis callidryas*) sampled from 12 sites along the Pacific coast of Costa Rica. Admixture proportions were generated using conStruct for K = 2–4 for both non-spatial and spatial models. Each bar represents an individual. The color of the bar shows the proportion of the individual's genome that is assigned to each of K layers.

2A, Fig. 6). Red-eyed treefrogs are likely semi-continuously distributed across their range, yet we sampled at discrete sampling locations; this risks over-estimating genetic groups inferred using clustering models (Bradburd et al., 2018; Frantz et al., 2009; Meirmans, 2012). Therefore, we used conStruct to compare models of population structure with and without spatial information (Bradburd et al., 2018). Comparing spatial and nonspatial models in conStruct indicated that most of the clustering observed in the nonspatial models arose from IBD (Fig. 7). Our results highlight the importance of considering patterns of IBD as they relate to genetic relatedness among discrete sampling sites: we would have over-estimated the genetic clustering of red-eyed treefrogs and come to strikingly different conclusions had we solely relied on nonspatial clustering models.

Spatial models show a division between the mainland and the two peninsular regions (Nicoya and Osa), but we assert that K=1 best describes the data because there is no *a priori* reason to expect that sites on the Nicoya and Osa peninsulas exchange migrants or share a more recent common ancestor with each other than with neighboring mainland sites. In fact, pairwise F_{ST} values between the Nicoya site and Osa sites are among the highest found in the dataset (Table 3, 0.408-0.415). Further, the non-spatial model did not support shared ancestry between Nicoya and Osa.

On both the Nicoya and Osa peninsulas, we expected red-eyed treefrogs to be isolated from neighboring sites on the mainland. Site 1 at the tip of the Nicoya Peninsula is one of the

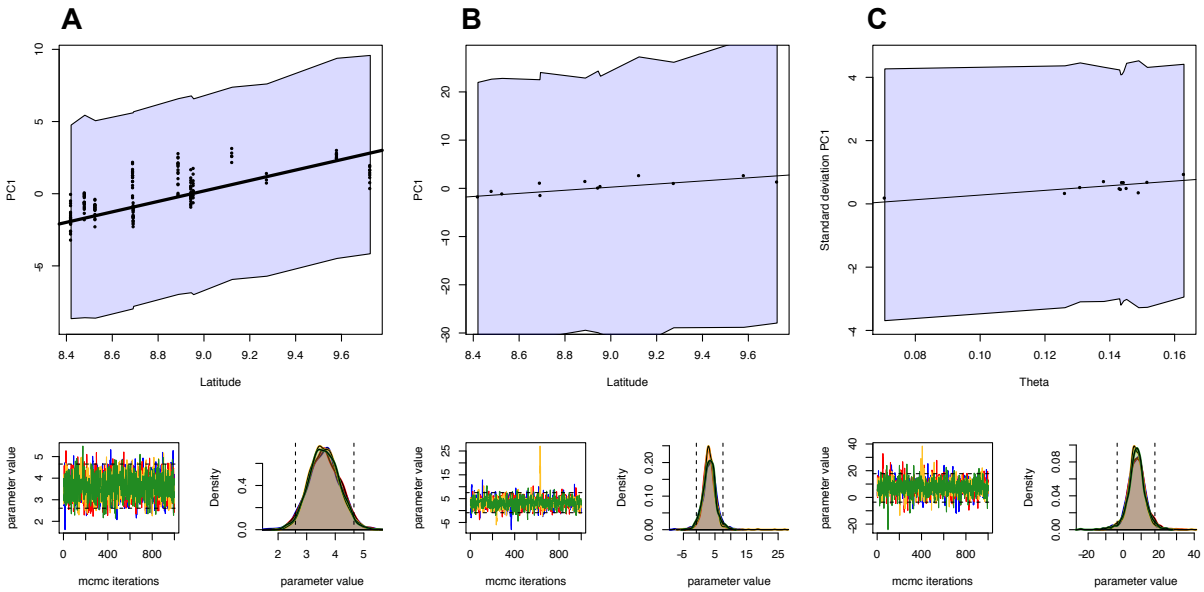

Figure 8. Results of Bayesian models with Dunn-Bonferroni corrected credible intervals (CI) showing the relationships between (A) latitude and PC1, (B) latitude and average PC1 value per site, and (C) Watterson's theta and variation in PC1 at each site. Each model contains genetic covariance as a covariate. Bolded line indicates that the 95% CI did not overlap with zero. Insets below model fit show estimated parameter values for 5,000 Markov chain Monte Carlo iterations.

only known populations of red-eyed treefrogs in the region, as dry forests unsuitable for red-eyed treefrogs cover most of far northwestern Costa Rica, including the Nicoya Peninsula (Kohlmann et al., 2002; Savage, 2002). The Osa Peninsula is genetically isolated from mainland sites for many taxa, including snakes and other frogs (Crawford, 2003; Crawford et al., 2007; Zamudio & Greene, 1997). However, we did not detect this pattern in red-eyed treefrogs on either peninsula once the geographic distance between mainland and peninsular sites was accounted for. Rather we found that red-eyed treefrogs on the Nicoya and Osa peninsulas are separated from mainland sites only due to IBD, rather than a mainland/peninsular barrier. This is particularly surprising for the Nicoya Peninsula, as dry forest is a clear barrier to red-eyed treefrog dispersal. It is possible that populations that persist along the coast (e.g., Gonzalez, 2013) provide a path for gene flow between the Nicoya and mainland sites.

Polymorphic patterns: Genetic introgression does not underlie color pattern polymorphism

We tested whether color-pattern polymorphism at a site arose through genetic introgression of divergent parent populations, the retention of ancestral polymorphism and/or ancient secondary contact (Fig. 2B). We did not find evidence of discrete parental groups, or recent introgression in the Central 2 region, despite patterns of color-pattern polymorphism (Table 2, Fig. 2,3). Rather our findings support that either color-pattern polymorphism was retained from an ancestral population, there has been ancient secondary contact, or that novel morphs have been generated by new mutations (Fig. 2B). Lab-bred hybrids provided examples of admixed ancestry and were the result of crossing orange and purple morph parents from geographically distant locations. It is likely that these parents were more genetically differentiated than the wild-caught orange and purple morph individuals living in the transition zone. Orange and purple frogs to the north,

south, and within the transition zone were assigned to similar genetic groups in both our spatial and nonspatial conStruct analyses, eliminating the possibility of genetic hybrids. Genetic IBD (Fig. 6), suggests that gene flow among sites is uninhibited by geographic barriers or other forms of premating reproductive isolation.

The distribution of color-pattern variation on the Pacific slope of Costa Rica seemingly mirrors patterns on the Caribbean: color-pattern polymorphism is found at a contact zone between two morphs. However, polymorphism in the Caribbean is the result of introgression between two distinct genetic groups of different color morphs (Akopyan et al., 2020b). There, red and blue morph frogs meet in a contact zone and produce frogs with a novel purple color pattern. Our contrasting findings for the Pacific slope emphasize that diverse evolutionary forces can produce similar patterns of phenotypic variation within intraspecific lineages. Whereas there is direct evidence that polymorphism on the Caribbean coast is the result of hybridization, the lack of recent genetic introgression along the Pacific slope suggests that variation in leg phenotype could have arisen due to the retention of ancestral color-pattern polymorphism in the region (as in Corl, Davis, Kuchta, & Sinervo, 2010), or ancient secondary contact (as in Lim et al., 2010). Additionally, polymorphism could be generated by novel mutations (as in Rosenblum et al., 2006, 2010).

Table 3. Pairwise F_{ST} (below diagonal) and geographic distance in kilometers (above diagonal) for 12 sampling sites along the Pacific coast of Costa Rica. Lines denote regional boundaries.

	Nicoya	North	Central 1		Central 2			Osa			South	
	1	2	3	4	5	6	7	8	9	10	11	12
1		212.2	299.4	323.5	350.6	354.4	359.1	385.4	410.7	412.8	396.7	439.3
2	0.286		89.3	113.2	139.9	143.9	148.5	168.8	193.6	189.1	186.1	215.8
3	0.422	0.163		24.2	51.4	55.2	60.1	80.2	104.9	100.5	97.6	127.2
4	0.419	0.206	0.075		27.2	31.0	35.9	56.1	80.8	76.4	73.4	103.1
5	0.394	0.231	0.099	0.058		4.3	8.8	29.9	54.6	50.2	46.3	76.0
6	0.393	0.250	0.126	0.088	0.069		6.3	28.2	52.9	48.5	42.4	72.3
7	0.382	0.235	0.107	0.070	0.054	0.033		22.1	46.9	42.5	37.9	67.3
8	0.415	0.272	0.168	0.137	0.126	0.115	0.090		25.4	21.4	38.4	66.9
9	0.408	0.270	0.168	0.139	0.129	0.119	0.092	0.036		21.5	60.4	89.5
10	0.412	0.274	0.172	0.143	0.134	0.124	0.097	0.031	0.025		55.0	84.1
11	0.411	0.273	0.156	0.116	0.095	0.075	0.059	0.122	0.127	0.131		32.5
12	0.412	0.279	0.166	0.125	0.104	0.082	0.066	0.130	0.135	0.139	0.039	

Spatial patterns of phenotype and genotype explained by multiple processes

Patterns of phenotypic and genetic variation permit us to test hypotheses about the evolutionary forces that influence lineage divergence. We found that genetic relatedness corresponds with phenotypic similarity in some regions of the Pacific coast, but not in others. These results highlight the complexity and nuance of this natural system, where multiple processes potentially shape diversity at a fine spatial scale, including genetic drift, selection, and ancient evolutionary history.

Red-eyed treefrogs on the Nicoya peninsula are isolated from the mainland by both geographic distance and tropical dry forests (see above), suggesting that genetic and phenotypic

differentiation in this region could have resulted from genetic drift. Evolution via drift is a common pattern for insular populations (e.g., Knopp et al., 2007, Lehtonen et al., 2009). Indeed, the Nicoya peninsula had the highest pairwise F_{ST} values to sampled populations at other locations (Table 3), and the lowest nucleotide diversity (Table 1). Individuals from the Nicoya Peninsula have a distinct, brighter orange phenotype then mainland frogs. In this case, the genetic and phenotypic divergence between the Nicoya and the mainland correspond, suggesting that drift could have resulted in both genetic and phenotypic differentiation.

In other instances, we found phenotypic changes are not well explained by neutral genetic relatedness at our genotyped loci, supporting the hypothesis that color pattern evolves through selection in this region (see below for discussion of selection). Along mainland coastal sites, we found a strong pattern of genetic IBD but a relatively weak pattern of phenotypic divergence with geographic distance across the entire Pacific coast, and a weak relationship between genetic distance and phenotypic distance (Fig. 6). Because geographic distance and color pattern both largely change along a latitudinal cline, it is difficult to decouple phenotypic changes from patterns of genetic IBD. We therefore used Bayesian models to test whether color-pattern phenotype changes more than expected given genetic relatedness, and, if so, whether that change is correlated with latitude. Both models found significant effects of latitude for PC1 and leg saturation and hue, but not for brightness measures (Fig. 8, Suppl. Fig. 2, 3). The relationship between phenotype and latitude disappeared at the site level, possibly due to reduced sample size. Given this result, we expect to find instances along the Pacific coast where color-pattern changes despite a high degree of genetic relatedness.

There are several instances along the Pacific coast where we observed changes in phenotype without corresponding changes in genetic deme. Orange and purple morph frogs along the mainland coast were not part of separate genetic demes, and instead conformed well to the coast-wide pattern of genetic IBD. Additionally, frogs from the polymorphic Central 2 region (Sites 5–7) and South (Sites 11–12) were assigned to the same genetic groups using both spatial and nonspatial clustering models (Fig. 7) and had low pairwise F_{ST} values (Table 3), despite different phenotypes (Table 2; Fig. 3). These incongruences between genetic patterns and phenotype suggest that phenotypic differences are maintained by selection despite the presence of gene flow.

We found additional incongruent patterns of variation on the Osa Peninsula. While all sites sampled within the Osa Peninsula were genetically similar and assigned to the same discrete genetic cluster (Fig. 4, 7), they were phenotypically distinct from one another (Table 2). Whether these are novel mutations, ancestral polymorphisms and/or the result of genetic drift in these relativity isolated and small populations remains unknown. Phenotypic divergence, despite genetic homogeneity, is a common pattern in nature, and usually has been attributed to sexual selection or adaptation to environmental variation. Some examples include *Epipedobates* poison frogs in Peru and Colombia (Tarvin et al., 2017), mimic poison frogs in Peru (Twomey et al., 2013) and redpoll finches in the Arctic circle (Mason & Taylor, 2015). The phenotypic variation on the Osa peninsula is particularly surprising given their small geographic scale (distance among sites ranges from 20–33 km).

As reported above, the transition in phenotype from orange legs to purple legs is not the result of two genetic demes meeting at a contact zone. It is possible that it was facilitated by ancient secondary contact between ancestral demes, one with orange flanks and legs and the other with purple flanks and legs. Frogs from the southern sites (7-12) and the Osa peninsula are part of a different mtDNA clade (clade A, Table 1) from the north (clade B; Table 1; Robertson

and Zamudio 2009). This biogeographic discordance between mtDNA and nuclear loci suggests past secondary contact (as in Toews & Brelsford, 2012). Along the mainland Pacific slope, frogs belong to the same genetic cluster, but have different mitochondrial haplotypes and distinct color patterns. This suggests that ancestral mitochondrial groups and color-pattern divergence have been maintained over time, whereas nuclear structure has been lost as a result of gene flow. Testing this hypothesis would require additional genomic data from these regions.

Role and mechanisms of selection

A nuanced set of selective pressures likely underlie the genetic and phenotypic patterns observed between and within red-eyed treefrog populations. Although hidden during the day when the frogs are at rest, the flanks and legs of red-eyed treefrogs are visible during activity at night, including during mating aggregations (Pyburn, 1970). Color pattern serves as a species and population-recognition cue in mate choice (Kaiser et al., 2018; Robertson & Greene, 2017). Mate preference for local color pattern has been demonstrated in this species, suggesting a role of sexual selection. Females from Site 2 and Site 12 have a preference for males with their local color pattern in mate-choice trials (Akopyan et al., 2018; Jacobs et al., 2016). Frogs from these sites also have distinguishable male calls and exhibit differences in female courtship behaviors (Akopyan et al., 2018), suggesting that preference for male traits could maintain local color-pattern differences despite the presence of gene flow.

Other forms of selection could also shape geographic variation in color pattern. Red-eyed treefrogs secrete noxious host-defense polypeptides from their skin (Conlon et al., 2007; Davis et al., 2016; Mignogna et al., 1997; Sazima, 1974), presenting the possibility that flank- and leg-color patterns act as aposematic signals to visual predators (Robertson & Greene, 2017). Geographic variation in host-defense polypeptides is correlated with color pattern in red-eyed treefrogs, indicating a role for ecological selection (Davis et al. 2016, Clark in prep.). Aposematic coloration is common among other brightly colored anurans (e.g., many species within Dendrobatidae, Mantellidae), and has been shown to vary among and within populations (Klonoski et al., 2019; Maan & Cummings, 2008; Rojas et al., 2014; Roland et al., 2017; Summers & Clough, 2001; Tarvin et al., 2017). Variation in the color pattern of aposematic species is often attributed to the interplay between ecological and sexual selection (Maan & Cummings, 2008; Nokelainen et al., 2012; Rojas & Endler, 2013). Future studies of red-eyed treefrogs that test the role of color pattern in predator avoidance would inform how ecological and sexual selective pressures interact to shape color-pattern distribution.

Conclusions

Our results highlight the complex evolutionary dynamics that shape color pattern in natural systems. We found that, despite a dramatic and discrete phenotypic change from orange to purple morphs, genetic variation in our study region follows a continuous pattern of IBD. Phenotypic polymorphism at sites located where the orange morph transitions to purple cannot be explained by recent hybridization as the orange and purple morphs are not genetically differentiated groups. Through the comparison of color pattern and genetic relatedness, we found evidence that indicates that selective forces have likely maintained color-pattern divergence in some regions, while genetic drift may play a role in others. Understanding the relative strength of sexual and ecological selection on color pattern is a logical next step for this system.

Acknowledgements

We thank K. Kaiser and R.E. Espinoza for help in developing the project and improving the manuscript, and Sirena Biological Station and the Firestone Center for Restoration Ecology for access to their properties for sampling. This work was supported by the Department of Biology and Research and Sponsored Projects at California State University, Northridge (CSUN), the CSUN Associated Students Scholarship in Honor of Jolene Koester, and a CSUN tuition waiver. This study was conducted in accordance with the current laws of Costa Rica and with approval of the Sistema Nacional de Áreas de Conservación of the Ministerio de Ambiente y Energía of Costa Rica (research and export permits R-053-2015 and 2015-CR1678). All procedures involving animals were approved by the California State University, Northridge Institutional Animal Care and Use Committee (IACUC 1819-005 and 1415-007a).

References

Abràmoff, M. D., Magalhães, P. J., & Ram, S. J. (2005). Image processing with ImageJ. *Biophotonics International*, *11*(7), 36–43. https://doi.org/10.1117/1.3589100

Akopyan, M., Gompert, Z., Klonoski, K., Vega, A., Kaiser, K., Mackelprang, R., Rosenblum, E. B., & Robertson, J. M. (2020a). *Genetic and phenotypic evidence of a contact zone between divergent color morphs of the iconic red-eyed treefrog*. [figshare]. Retrived from: https://doi.org/https://doi.org/10.6084/m9.figshare.11923017.v2

Akopyan, M., Gompert, Z., Klonoski, K., Vega, A., Kaiser, K., Mackelprang, R., Rosenblum, E. B., & Robertson, J. M. (2020b). Genetic and phenotypic evidence of a contact zone between divergent colour morphs of the iconic red-eyed treefrog. *Molecular Ecology*, *29*(22), 4442–4456. https://doi.org/10.1111/mec.15639

Akopyan, M., Kaiser, K., Vega, A., Savant, N. G., Owen, C. Y., Dudgeon, S. R., & Robertson, J. M. (2018). Melodic males and flashy females: Geographic variation in male and female reproductive behavior in red-eyed treefrogs (*Agalychnis callidryas*). *Ethology*, *124*(1), 54–64. https://doi.org/10.1111/eth.12705

Ali, O. A., O'Rourke, S. M., Amish, S. J., Meek, M. H., Luikart, G., Jeffres, C., & Miller, M. R. (2016). RAD capture (rapture): Flexible and efficient sequence-based genotyping. *Genetics*, *202*(2), 389–400. https://doi.org/10.1534/genetics.115.183665

Anderson, E., & Stebbins, G. L. (1954). Hybridization as an evolutionary stimulus. *Evolution*, *8*(4), 378–388. https://doi.org/10.2307/2405784

Bradburd, G. S., Coop, G. M., & Ralph, P. L. (2018). Inferring continuous and discrete population genetic structure across space. *Genetics*, *210*(1), 33–52. https://doi.org/10.1534/genetics.118.301333

Bradburd, G. S., Ralph, P. L., & Coop, G. M. (2013). Disentangling the effects of geographic and ecological isolation on genetic differentiation. *Evolution*, *67*(11), 3258–3273. https://doi.org/10.1111/evo.12193

Campbell, J. (1999). Distribution patterns of amphibians in Middle America. In W. Duellman (Ed.), *Patterns of Distribution of Amphibians*. The John Hopkins University Press.

Catchen, J., Hohenlohe, P. A., Bassham, S., Amores, A., & Cresko, W. A. (2013). Stacks: An analysis tool set for population genomics. *Molecular Ecology*, *22*(11), 3124–3140.

Chessel, D., Dufour, A. B., & Thioulouse, J. (2004). The ade4 package-1: One-table methods. *R News*, *4*(1), 5–10.

Conlon, J. M., Woodhams, D. C., Raza, H., Coquet, L., Leprince, J., Jouenne, T., Vaudry, H., &

Rollins-Smith, L. A. (2007). Peptides with differential cytolytic activity from skin secretions of the lemur leaf frog *Hylomantis lemur* (Hylidae: Phyllomedusinae). *Toxicon*, *50*(4), 498–506.

Corl, A., Davis, A. R., Kuchta, S. R., & Sinervo, B. (2010). Selective loss of polymorphic mating types is associated with rapid phenotypic evolution during morphic speciation. *Proceedings of the National Academy of Sciences*, *107*(9), 4254–4259. https://doi.org/10.1073/pnas.0909480107

Cott, H. B. (1940). *Adaptive coloration in animals*. Metheun and Co. Ltd.

Crawford, A. J. (2003). Huge populations and old species of Costa Rican and Panamanian dirt frogs inferred from mitochondrial and nuclear gene sequences. *Molecular Ecology*, *12*(10), 2525–2540.

Crawford, A. J., Bermingham, E., & Polania, C. (2007). The role of tropical dry forest as a long-term barrier to dispersal: A comparative phylogeographical analysis of dry forest tolerant and intolerant frogs. *Molecular Ecology*, *16*(22), 4789–4807.

Cummings, M. E., & Crothers, L. R. (2013). Interacting selection diversifies warning signals in a polytypic frog: An examination with the strawberry poison frog. *Evolutionary Ecology*, *27*(4), 693–710. https://doi.org/10.1007/s10682-013-9648-9

Davis, L. R., Klonoski, K., Rutschow, H. L., Van Wijk, K. J., Sun, Q., Haribal, M. M., Saporito, R. A., Vega, A., Rosenblum, E. B., Zamudio, K. R., & Robertson, J. M. (2016). Host defense skin peptides vary with color pattern in the highly polymorphic red-eyed treefrog. *Frontiers in Ecology and Evolution*, *4*, 97–112. https://doi.org/10.3389/fevo.2016.00097

Duftner, N., Sefc, K. M., Koblmüller, S., Nevado, B., Verheyen, E., Phiri, H., & Sturmbauer, C. (2006). Distinct population structure in a phenotypically homogeneous rock-dwelling cichlid fish from Lake Tanganyika. *Molecular Ecology*, *15*(9), 2381–2395. https://doi.org/10.1111/j.1365-294X.2006.02949.x

Endler, J. A. (1973). Gene flow and population differentiation. *Science*, *179*(4070), 243–250. https://doi.org/10.1126/science.179.4070.243

Etter, P. D., Preston, J. L., Bassham, S., Cresko, W. A., & Johnson, E. A. (2011). Local *de novo* assembly of RAD paired-end contigs using short sequencing reads. *PLoS ONE*, *6*(4). https://doi.org/10.1371/journal.pone.0018561

Frantz, A. C., Cellina, S., Krier, A., Schley, L., & Burke, T. (2009). Using spatial Bayesian methods to determine the genetic structure of a continuously distributed population: Clusters or isolation by distance? *Journal of Applied Ecology*, *46*(2), 493–505. https://doi.org/10.1111/j.1365-2664.2008.01606.x

Gompert, Z., & Buerkle, C. A. (2016). What, if anything, are hybrids: Enduring truths and challenges associated with population structure and gene flow. *Evolutionary Applications*, *9*(7), 909–923. https://doi.org/10.1111/eva.12380

Gompert, Z., Lucas, L. K., Buerkle, C. A., Forister, M. L., Fordyce, J. A., & Nice, C. C. (2014). Admixture and the organization of genetic diversity in a butterfly species complex revealed through common and rare genetic variants. *Molecular Ecology*, *23*(18), 4555–4573.

Gonzalez, K. (2013). *Agalychnis callidryas*, Range extension. *Herpetological Bulletin*, *125*, 25–33.

Hoekstra, H. E., Drumm, K. E., & Nachman, M. W. (2004). Ecological genetics of adaptive color polymorphism in pocket mice: Geographic variation in selected and neutral genes. *Evolution*, *58*(6), 1329–1341. https://doi.org/10.1111/j.0014-3820.2004.tb01711.x

Jacobs, L. E., Vega, A., Dudgeon, S., Kaiser, K., & Robertson, J. M. (2016). Local not vocal:

583 assortative female choice in divergent populations of red-eyed treefrogs, *Agalychnis*
584 *callidryas* (Hylidae: Phyllomedusinae). *Biological Journal of the Linnean Society*, *120*(1),
585 171–178. https://doi.org/10.1111/bij.12861
586 Kaiser, K., Boehlke, C., Navarro-Pérez, E., Vega, A., Dudgeon, S., & Robertson, J. M. (2018).
587 Local preference encoded by complex signaling: Mechanisms of mate preference in the red-
588 eyed treefrog (*Agalychnis callidryas*). *Behavioral Ecology and Sociobiology*, *72*(12), 182.
589 https://doi.org/10.1007/s00265-018-2597-0
590 Klonoski, K., Bi, K., & Rosenblum, E. B. (2019). Phenotypic and genetic diversity in aposematic
591 Malagasy poison frogs (genus *Mantella*). *Ecology and Evolution*, *9*(5), 2725–2742.
592 https://doi.org/10.1002/ece3.4943
593 Knopp, T., Cano, J. M., Crochet, P. A., & Merila, J. (2007). Contrasting levels of variation in
594 neutral and quantitative genetic loci on island populations of moor frogs (*Rana arvalis*).
595 *Conservation Genetics*, *8*(1), 45–56. https://doi.org/10.1007/s10592-006-9147-4
596 Kohlmann, B., Wilkinson, J., & Lulla, K. (2002). *Costa Rica desde el espacio/Costa Rica from*
597 *Space* (1st ed.). Fundacíon Neotrópica.
598 Lehtonen, P. K., Laaksonen, T., Artemyev, A. V., Belskii, E., Both, C., Bureš, S., Bushuev, A.
599 V., Krams, I., Moreno, J., Mägi, M., Nord, A., Potti, J., Ravussin, P. A., Sirkiä, P. M.,
600 Sætre, G. P., & Primmer, C. R. (2009). Geographic patterns of genetic differentiation and
601 plumage colour variation are different in the pied flycatcher (*Ficedula hypoleuca*).
602 *Molecular Ecology*, *18*(21), 4463–4476. https://doi.org/10.1111/j.1365-294X.2009.04364.x
603 Li, H. (2011). A statistical framework for SNP calling, mutation discovery, association mapping
604 and population genetical parameter estimation from sequencing data. *Bioinformatics*,
605 *27*(21), 2987–2993. https://doi.org/10.1093/bioinformatics/btr509
606 Li, H., & Durbin, R. (2009). Fast and accurate short read alignment with Burrows–Wheeler
607 transform. *Bioinformatics*, *25*(14), 1754–1760.
608 Li, H., Handsaker, B., Wysoker, A., Fennell, T., Ruan, J., Homer, N., Marth, G., Abecasis, G., &
609 Durbin, R. (2009). The Sequence Alignment/Map format and SAMtools. *Bioinformatics*,
610 *25*(16), 2078–2079. https://doi.org/10.1093/bioinformatics/btp352
611 Lim, H. C., Sheldon, F. H., & Moyle, R. G. (2010). Extensive color polymorphism in the
612 southeast Asian oriental dwarf kingfisher *Ceyx erithaca*: A result of gene flow during
613 population divergence? *Journal of Avian Biology*, *41*(3), 305–318.
614 https://doi.org/10.1111/j.1600-048X.2009.04913.x
615 Lowry, D. B., Sheng, C. C., Lasky, J. R., & Willis, J. H. (2012). Five anthocyanin
616 polymorphisms are associated with an R2R3-MYB cluster in *Mimulus guttatus*
617 (Phrymaceae). *American Journal of Botany*, *99*(1), 82–91.
618 https://doi.org/10.3732/ajb.1100285
619 Maan, M. E., & Cummings, M. E. (2008). Female preferences for aposematic signal components
620 in a polymorphic poison frog. *Evolution*, *62*(9), 2334–2345. https://doi.org/10.1111/j.1558-
621 5646.2008.00454.x
622 Maan, M. E., Eshuis, B., Haesler, M. P., Schneider, M. V., Van Alphen, J. J. M., & Seehausen,
623 O. (2008). Color polymorphism and predation in a Lake Victoria cichlid fish. *Copeia*,
624 *2008*(3), 621–629. https://doi.org/10.1643/CE-07-114
625 Mason, N. A., & Taylor, S. A. (2015). Differentially expressed genes match bill morphology and
626 plumage despite largely undifferentiated genomes in a Holarctic songbird. *Molecular*
627 *Ecology*, *24*(12), 3009–3025. https://doi.org/10.1111/mec.13140
628 Mayr, E. (1963). *Animal species and evolution*. Harvard University Press.

629 Meirmans, P. G. (2012). The trouble with isolation by distance. *Molecular Ecology*, *21*(12),
630 2839–2846. https://doi.org/10.1111/j.1365-294X.2012.05578.x
631 Mignogna, G., Severini, C., Erspamer, G. F., Siciliano, R., Kreil, G., & Barra, D. (1997).
632 Tachykinins and other biologically active peptides from the skin of the Costa Rican
633 phyllomedusid frog *Agalychnis callidryas*. *Peptides*, *18*, 367–374.
634 Mitchell-Olds, T., Willis, J. H., & Goldstein, D. B. (2007). Which evolutionary processes
635 influence natural genetic variation for phenotypic traits? *Nature Reviews Genetics*, *8*(11),
636 845–856. https://doi.org/10.1038/nrg2207
637 Nokelainen, O., Hegna, R. H., Reudler, J. H., Lindstedt, C., & Mappes, J. (2012). Trade-off
638 between warning signal efficacy and mating success in the wood tiger moth. *Proceedings of*
639 *the Royal Society B: Biological Sciences*, *279*(1727), 257–265.
640 https://doi.org/10.1098/rspb.2011.0880
641 Orteu, A., & Jiggins, C. D. (2020). The genomics of coloration provides insights into adaptive
642 evolution. *Nature Reviews Genetics*, *21*(8), 461–475. https://doi.org/10.1038/s41576-020-
643 0234-z
644 Pfeifer, S. P., Laurent, S., Sousa, V. C., Linnen, C. R., Foll, M., Excoffier, L., Hoekstra, H. E., &
645 Jensen, J. D. (2018). The evolutionary history of Nebraska deer mice: Local adaptation in
646 the face of strong gene flow. *Molecular Biology and Evolution*, *35*(4), 792–806.
647 https://doi.org/10.1093/molbev/msy004
648 Planes, S., & Doherty, P. J. (1997). Genetic and color interactions at a contact zone of
649 *Acanthochromis polyacanthus*: A marine fish lacking pelagic larvae. *Evolution*, *51*(4), 1232.
650 https://doi.org/10.2307/2411052
651 Pujol, B., Wilson, A. J., Ross, R. I. C., & Pannell, J. R. (2008). Are QST-FST comparisons for
652 natural populations meaningful? *Molecular Ecology*, *17*(22), 4782–4785.
653 https://doi.org/10.1111/j.1365-294X.2008.03958.x
654 Pyburn, W. F. (1970). Breeding behavior of the leaf-frogs *Phyllomedusa callidryas* and
655 *Phyllomedusa dacnicolor* in Mexico. *Copeia*, 209–218.
656 Robertson, J. M., Duryea, M. C., & Zamudio, K. R. (2009). Discordant patterns of evolutionary
657 differentiation in two Neotropical treefrogs. *Molecular Ecology*, *18*(7), 1375–1395.
658 https://doi.org/10.1111/j.1365-294X.2009.04126.x
659 Robertson, J. M., & Greene, H. W. (2017). Bright colour patterns as social signals in nocturnal
660 frogs. *Biological Journal of the Linnean Society*, *121*(4), 849–857.
661 https://doi.org/doi:10.1093/jxb/eru508 1.5
662 Robertson, J. M., & Robertson, A. D. (2008). Spatial and temporal patterns of phenotypic
663 variation in a Neotropical frog. *Journal of Biogeography*, *35*(5), 830–843.
664 https://doi.org/10.1111/j.1365-2699.2007.01824.x
665 Robertson, J. M., & Vega, A. (2011). Genetic and phenotypic variation in a colourful treefrog
666 across five geographic barriers. *Journal of Biogeography*, *38*(11), 2122–2135.
667 https://doi.org/10.1111/j.1365-2699.2011.02548.x
668 Robertson, J. M., & Zamudio, K. R. (2009). Genetic diversification, vicariance, and selection in
669 a polytypic frog. *Journal of Heredity*, *100*(6), 715–731.
670 https://doi.org/10.1093/jhered/esp041
671 Rojas, B. (2016). Behavioural, ecological, and evolutionary aspects of diversity in frog colour
672 patterns. *Biological Reviews*, *92*(2), 1059–1080. https://doi.org/10.1111/brv.12269
673 Rojas, B., Devillechabrolle, J., & Endler, J. A. (2014). Paradox lost: Variable colour-pattern
674 geometry is associated with differences in movement in aposematic frogs. *Biology Letters*,

675 *10*(6), 20140193. https://doi.org/10.1098/rsbl.2014.0193
676 Rojas, B., & Endler, J. A. (2013). Sexual dimorphism and intra-populational colour pattern
677 variation in the aposematic frog *Dendrobates tinctorius. Evolutionary Ecology*, *27*(4), 739–
678 753. https://doi.org/10.1007/s10682-013-9640-4
679 Roland, A. B., Santos, J. C., Carriker, B. C., Caty, S. N., Tapia, E. E., Coloma, L. A., &
680 O'Connell, L. A. (2017). Radiation of the polymorphic Little Devil poison frog (*Oophaga*
681 *sylvatica*) in Ecuador. *Ecology and Evolution*, *7*(22), 9750–9762.
682 https://doi.org/10.1002/ece3.3503
683 Rosenblum, E. B., Hoekstra, H. E., & Nachman, M. W. (2006). Adaptive reptile color variation
684 and the evolution of the MC1R gene. *Evolution*, *58*(8), 1794. https://doi.org/10.1554/03-741
685 Rosenblum, E. B., Rompler, H., Schoneberg, T., & Hoekstra, H. E. (2010). Molecular and
686 functional basis of phenotypic convergence in white lizards at White Sands. *Proceedings of*
687 *the National Academy of Sciences of the United States of America*, *107*(5), 2113–2117.
688 https://doi.org/10.1073/pnas.0911042107
689 Savage, J. M. (2002). *The amphibians and reptiles of Costa Rica: A herptofauna between two*
690 *continents, between two seas* (Vol. 1). The University of Chicago Press.
691 Savage, J. M., & Heyer, W. R. (1967). Variation and distribution in the tree-frog genus
692 *Phyllomedusa* in Costa Rica, central America. *Beitrage Zur Neotropischen Fauna*, *5*(2),
693 111–131. https://doi.org/10.1080/01650526709360400
694 Sazima, I. (1974). Experimental predation on the leaf-frog *Phyllomedusa rohdei* by the water
695 snake *Liophis miliaris*. *Society for the Study of Amphibians and Reptiles*, *8*(4), 376–377.
696 Schliwa, M., & Euteneuer, U. (1983). Comparative ultrastructure and physiology of
697 chromatophores, with emphasis on changes associated with intracellular-transport.
698 *American Zoologist*, *23*(3), 479–494.
699 Selz, O. M., Thommen, R., MER, P., JM, A.-R., & Seehausen, O. (2016). Differences in male
700 coloration are predicted by divergent sexual selection between populations of a cichlid fish.
701 *Proceedings of the Royal Society Biological Sciences*, *283*(1830), 20160172.
702 https://doi.org/10.1098/rspb.2016.0172
703 Shirk, A. J., Landguth, E. L., & Cushman, S. A. (2017). A comparison of individual-based
704 genetic distance metrics for landscape genetics. *Molecular Ecology Resources*, *17*(6), 1308–
705 1317. https://doi.org/10.1111/1755-0998.12684
706 Slatkin, M. (1985). Gene flow in natural populations. *Annual Review of Ecology and*
707 *Systematics*, *16*(May), 393–430.
708 Stevens, M., & Merilaita, S. (2009). Animal camouflage: Current issues and new perspectives.
709 *Philosophical Transactions of the Royal Society. Series B, Biological Sciences*,
710 *364*(November 2008), 423–427. https://doi.org/10.1098/rstb.2008.0217
711 Streisfeld, M. A., & Kohn, J. R. (2005). Contrasting patterns of floral and molecular variation
712 across a cline in *Mimulus aurantiacus*. *Evolution*, *59*(12), 2548. https://doi.org/10.1554/05-
713 514.1
714 Summers, K., & Clough, M. E. (2001). The evolution of coloration and toxicity in the poison
715 frog family (Dendrobatidae). *Proceedings of the National Academy of Sciences, USA*,
716 *98*(11), 6227–6232.
717 Supple, M. A., Papa, R., Hines, H. M., McMillan, W. O., & Counterman, B. A. (2015).
718 Divergence with gene flow across a speciation continuum of Heliconius butterflies. *BMC*
719 *Evolutionary Biology*, *15*. https://doi.org/10.1186/s12862-015-0486-y
720 Svensson, E. I. (2017). Back to basics: using colour polymorphisms to study evolutionary

processes. *Molecular Ecology*, *26*(8), 2204–2211. https://doi.org/10.1111/mec.14025

Tarvin, R. D., Powell, E. A., Santos, J. C., Ron, S. R., & Cannatella, D. C. (2017). The birth of aposematism: High phenotypic divergence and low genetic diversity in a young clade of poison frogs. *Molecular Phylogenetics and Evolution*, *109*, 283–295. https://doi.org/10.1016/j.ympev.2016.12.035

Toews, D. P. L., & Brelsford, A. (2012). The biogeography of mitochondrial and nuclear discordance in animals. *Molecular Ecology*, *21*(16), 3907–3930. https://doi.org/10.1111/j.1365-294X.2012.05664.x

Twomey, E., Mayer, M., & Summers, K. (2015). Intraspecific call variation in the mimic poison frog *Ranitomeya imitator*. *Herpetologica*, *71*(4), 252–259.

Twomey, E., Yeager, J., Brown, J. L., Morales, V., Cummings, M., & Summers, K. (2013). Phenotypic and genetic divergence among poison frog populations in a mimetic radiation. *PLoS ONE*, *8*(2), e55443. https://doi.org/10.1371/journal.pone.0055443

Wang, I. J., & Summers, K. (2010). Genetic structure is correlated with phenotypic divergence rather than geographic isolation in the highly polymorphic strawberry poison-dart frog. *Molecular Ecology*, *19*(3), 447–458. https://doi.org/10.1111/j.1365-294X.2009.04465.x

Watterson, G. A. (1975). On the number of segregating sites in genetical models without recombination. *Theoretical Population Biology*, *7*(2), 256–276. https://doi.org/10.1039/b316709g

Weir, B. S., & Hill, W. G. (2002). Estimating F-statistics. *Annual Review of Genetics*, *36*(1), 721–750. https://doi.org/10.1146/annurev.genet.36.050802.093940

Zamudio, K. R., & Greene, H. W. (1997). Phylogeography of the bushmaster (*Lachesis muta*: Viperidae): Implications for neotropical biogeography, systematics, and conservation. *Biological Journal of the Linnean Society*, *62*(3), 421–442.

Data Accessibility

Raw data, input files, and scripts will be available on figshare.com. This section will be updated with doi information upon completion.

Author Contributions

MIC, JMR, MA, EBR and AV designed this study. JMR, MA, and AV carried out field sampling. MIC performed phenotypic analyses, library preparation and bioinformatics. GSB and MIC carried out statistical and computational modeling. Funding support from JMR, EBR, MIC. MIC drafted the manuscript, and all authors have contributed to and approved the final version.